On Pellet Ablation in Hot Plasmas and the Problem of Magnetic Shielding

L. L. Lengyel

IPP 4/160 April 1977

MAX-PLANCK-INSTITUT FÜR PLASMAPHYSIK

8046 GARCHING BEI MÜNCHEN

MAX-PLANCK-INSTITUT FÜR PLASMAPHYSIK

GARCHING BEI MÜNCHEN

On Pellet Ablation in Hot Plasmas and the Problem of Magnetic Shielding

L. L. Lengyel

IPP 4/160 April 1977

Die nachstehende Arbeit wurde im Rahmen des Vertrages zwischen dem Max-Planck-Institut für Plasmaphysik und der Europäischen Atomgemeinschaft über die Zusammenarbeit auf dem Gebiete der Plasmaphysik durchgeführt.

IPP 4/160

On Pellet Ablation in Hot Plasmas and the Problem of Magnetic Shielding.

L.L. Lengyel

April 1977

Abstract

Theories published on pellet ablation phenomena are reviewed. Some inconsistencies are shown to exist in some of the studies available. Models are developed and estimates are given for pellet ablation rates in hot plasmas with and without magnetic fields present. The possible existence of a self-regulating ablation mechanism is indicated.

The injection of frozen hydrogen-isotope pellets in hot plasmas in considered as a possible means of increasing the plasma density in present tokamak experiments [1, 2] and for replanishing particle losses in the next generation of tokamak installations. The ultimate purpose of pellet injection experiments is the development of a method for the cold refueling of future reactor-size CTR experiments. The idea of refueling by means of pellet injection originates from Spitzer and co-workers [3]. The alternative refueling methods (gas bleed-in, neutral injection, cluster injection) as applied to reactor-size experiments either lead to ionization and particle capture at the plasma boundary, thus generating inverted density profiles, or require very high injection energies to ensure penetration times shorter than the ionization time of the particles. Acceleration of a large number of particles to the required velocity (typically 5×10^{12} particles/s per watt reactor output

are considered to be the necessary refueling rate [4]) would require prohibitively large and expensive injector installations. The injection power requirements are somewhat relaxed if cluster injection is considered [5], but only pellet injection with estimated injection velocities of the order of 10^4 m/s (approx. 1 eV of energy per particle) offers a real alternative. The magnitude of the required injection velocity is determined in this case by the estimated ablation rates.

Pellet ablation in a hot plasma is affected by a number of physical phenomena. The surface of a pellet exposed suddenly to a plasma is bombarded directly by the plasma particles until the ablation products form a protective blanket around it. Some of the electrons impinging on the pellet surface are subject to elastic scattering, the rest undergo excitational and ionizational collisions. The higher the energy of the incident electrons the higher is the number of ionizing events [6], while the energy transferred to an ion pair produced approaches an asymptotic value. At the same time, the electrons transfer momentum to the pellet. Also the ions impinging on the pellet surface transfer momentum and energy to it. The ions may be subject to charge exchange collisions: the backscattered hot neutrals are then ionized by the surrounding plasma and the cold ions left behind increase the degree of ionization of the pellet mass. With time the ablation products form a moderately warm plasma blanket around the pellet,which may be partially or fully ionized, depending upon the energy flux to the pellet. The blanket, heated at its outer boundary by the surrounding plasma and cooled at its inner boundary by the pellet, shields

the pellet,partially or totally, from the incident hot plasma particles and acts, at the same time, as a heat reservoir for the pellet itself. There is thus a continuous exchange of mass, momentum and energy at the pellet-blanket and blanket--plasma interfaces, resulting in a continuous phase transition from the condensed phase to ionized matter.

In this paper, we are concerned primarily with the first phase of the ablation process, i.e. the determination of the blanket parameters and the resulting ablation rates as functions of the incident energy flux. If the parameters of the surrounding plasma are given, the momentum and energy fluxes incident on the pellet surface can be estimated in the absence of shielding by

$$\dot{p} \approx \frac{1}{4} n_e v_{eth} (m_e v_{eth}) + \frac{1}{4} n_i v_{ith} (m_i v_{ith}), \qquad (0.1)$$

$$\phi \approx \frac{1}{4} n_e v_{eth} (\frac{3}{2} kT_e) + \frac{1}{4} n_i v_{ith} (\frac{3}{2} kT_e), \qquad (0.2)$$

where $v_{th} = (8\ kT/\pi m)^{1/2}$; and $T_i \approx T_e$.

Hence, while electrons and ions play an equal role in the transfer of momentum, energy is transported primarily by the electrons. If the incident electrons have a Maxwellian distribution, it can be shown by integrating over all electron energies [6, 8] that

$$\Phi \approx \frac{1}{2} n_e v_{eth} (kT_e). \qquad (0.3)$$

Since the electron thermal velocity under experimental conditions of practical interest is likely to be much higher than the pellet injection velocity, the heating of the

pellet by the incident particles can be considered as spherically symmetric and the effect of the pellet motion on the ablation process may be neglected. (The effect of a magnetic field has not yet been considered.) Hence the phase transition time associated with the sublimation or ionization of the pellet can readily be estimated in a "zero-dimensional" approximation by writing the energy balance for a spherical pellet heated uniformly over its surface:

$$4 \pi r_p^2 \Phi \Delta t = \frac{4}{3} \pi r_p^3 n_c \epsilon_{ph}, \qquad (0.4)$$

where r_p is the pellet radius, n_c the particle density of the condensed phase, and ϵ_{ph} the phase transition energy per particle. Hence the ablation time Δt, the average ablation front velocity $u = r_p / \Delta t$, and the mass flux $\dot{m} = u \rho_c$ can readily be expressed as functions of the incident energy flux ($\rho_c = m_a n_c$, m_a is the atomic mass):

$$\Delta t = \frac{1}{3} n_c r_p \epsilon_{ph} / \Phi \ , \ u = 3\Phi / n_c \epsilon_{ph}, \text{ and } \dot{m} = 3 m_a \Phi / \epsilon_{ph}. \qquad (0.5)$$

Note that the ablation front velocity and the mass flux in this approximation are directly proportional to Φ. Taking typical reactor plasma conditions and pellet parameters ($n_e \approx 10^{14}$ cm^{-3}, $T \simeq 10$ keV, $\Phi \approx 10^{13}$ W/m^2, $n_c \simeq 5 \times 10^{22}$ cm^{-3}, $r_p \approx 1$ cm, $\epsilon_{ph} = 0.005$ eV and 36.2 eV for sublimation and for producing a hydrogen ion pair [7], respectively) we have $\Delta t_{subl} \approx 1.4 \times 10^{-7}$ s, and $\Delta t_{ioniz} \approx 10^{-4}$ s, respectively.

Hence if the pellet is to penetrate a plasma column with a minor radius of a $\geq$ 1 m without being fully ionized, an injection velocity of the order of 10^4 m/s and higher would be required.

The assumption of instantaneous phase transition at the pellet surface is well justified for the vaporization (sublimation) process, but it may yield incorrect rates for the ionization process, particularly at low plasma temperatures. Indeed, if the energy flux is not sufficient for instantaneous ionization at the pellet surface, the vaporized material may form a cold cloud around the pellet, thus increasing the surface area exposed to the incident energy flux. The radius of this could can be estimated if the expansion velocity of the ablated particles and the time required for their ionization are known:

$$r_{vap} \simeq v_{vap}\, \Delta t_i ; \text{ where } \Delta t_i = \Delta t_i(n_e, T_e). \qquad (0.6)$$

Assuming free expansion in vacuum

$$(\gamma kT_c/m)^{1/2} \lesssim v_{vap} \lesssim (4\gamma\varepsilon/(\gamma-1)m)^{1/2} \qquad (0.7)$$

where ε/m is the energy per unit mass imparted to the pellet and is of the order of the sublimation energy (0.005 eV) per particle mass. The ionization time may then be compared with the value that can be obtained from equ. (0.5) by allowing for the increased effective surface:

$$\Delta t = \frac{1}{3}\, n_c r_p \varepsilon_i \Phi^{-1} \left(r_p/r_{vap}\right)^2 \qquad (0.8)$$

Experiments performed on the Pulsator Tokamak at Garching[2] yielded ablation times of the order of 300 μs for deuterium pellets approx. 0.6 mm in size at plasma parameter values of $n_e \approx 10^{13}$ cm^{-3}, $T_e < 10$ eV ($\phi \lesssim 2.0 \times 10^7$ W/m^2). The time-resolved electron density measurements showed that the ionization of the pellet mass was completed by the end of the ablation process. The H_α line emission indicated the presence of a cloud approx. 5 cm in radius around the pellet. For the above plasma parameters equs. (0.5) to (0.8) yield $\Delta t_{vap} \approx 280$ μs, $\Delta t_i \approx 50$ μs, $262 < v_{vap} < 1500$ m/s, $r_{vap} \lesssim 8$ cm, and $\Delta t \approx 320$ μs ($T_c \approx 10^{o}$K).

Note that in the above approximation the energy expended on raising the kinetic and internal energies of the ablation products has been completely neglected. The flux reduction caused by the presence of the gas blanket around the pellet and the effect of the finite penetration depths of the incident particles [8] have not been taken into account either. A further significant reduction of the ablation rates may be caused by possible electrostatic and magnetic shielding.

Electrostatic shielding may take place if the pellet is negatively charged by the incident electrons. The magnitude of this effect is determined by secondary emission phenomena, i.e. by the number of electrons emitted per incident electron. The secondary emission coefficients is a function of the incident electron energy and of the target material; and it may be greater or less than unity. Condensed hydrogen isotope pellets may be treated as dielectrics. However, the secondary emission process is coupled in our case with the process of removal of molecular layers from the pellet surface owing to vaporization. The net effect of these simultaneous processes has not yet geen investigated and is beyond the scope of this analysis.

Magnetic shielding is caused by the reduction of the effective plasma transport properties across the magnetic field. If $\omega_{ci}\tau_{ii} >> 1$ (ω_{ci} and τ_{ii} denote the ion cyclotron frequency and the ion-ion collision time), the thermal conductivity of a plasma along the magnetic field lines is dominated by electron conduction, while that across the field lines is dominated by ion conduction, owing to the larger Larmor radii of the ions. Chang [7] has shown that the thermal flux carried by the ions along and across the magnetic field lines are

$$\phi_{\parallel}^{i} \approx 1.3\, n_i v_{ith}\, (kT_i) \quad \text{and} \quad \phi_{\perp}^{i} \approx 0.67\, v_{ith}\, n_i kT_i/(\omega_{ci}\tau_{ii}),$$

respectively. Hence, since $\phi_{\parallel}^{e} > \phi_{\parallel}^{i}$ ($\varkappa_e / \varkappa_i \sim (m_i/m_e)^{1/2}$), it follows that $\phi_{\perp}^{i}/\phi_{\parallel}^{e} < \phi_{\perp}^{i}/\phi_{\parallel}^{i} \approx (\omega_{ci}\tau_{ii})^{-1}$. Since $(\omega_{ci}\tau_{ii}) >> 1$ for most cases of practical interest, one has $\phi_{\parallel}^{e} >> \phi_{\perp}^{e} + \phi_{\perp}^{i}$. Hence, if no anomalous transport processes are present, only the energy flux transported by the electrons along the magnetic field lines play an essential role, and the pellet with its surrounding blanket is not exposed to a spherically symmetric energy influx.

The ablation of deuterium pellets in hot plasmas in the absence of magnetic fields was considered by Gralnick [8]. The results he obtained from a steady-state ablation wave model were used as inner boundary conditions in subsequent numerical calculations pertaining to the expansion dynamics of the ablated material. (The outer boundary conditions were given by the fusion plasma parameters.) The magnetic shielding effect was considered by Rose [5] in a steady-state spherically symmetric magneto-static approximation. The gas blanket surrounding the pellet was assumed here to be fully ionized and field-free. Chang[7] has proposed a flexible magnetic nozzle model in which he allowed for field penetration into the plasma and plasma motion along the magnetic field lines.

Some of the assumptions made in the above analyses shall be re-examined and corrected in the present work and thus some aspects of the above models shall still be discussed in detail. Ablation rates based on properly defined mathematical models shall be calculated here both in the absence of magnetic fields and with magnetic fields present.

1. ABLATION KINETICS IN THE ABSENCE OF MAGNETIC FIELD

1.1 Gralnick's Model

Gralnick [8] has analyzed the ablation of deuterium condensate in a hot plasma by means of a one-dimensional plane wave approximation using the ideal gas conservation equations. His model consists of two phases: the undisturbed condensed phase and the vaporized phase. The two phases are separated by the vaporization front, in which the energy flux Φ transported by the plasma particles is deposited. The solid phase is at rest in a laboratory frame of reference, the ablation front moves into the condensate with a velocity u_ϕ. In a reference frame moving with the ablation front the conservation equations can be written in the following form (see Fig. 1):

$$\dot{m} = \rho_c v_c = \rho_1 v_r \quad , \tag{1.1}$$

$$\dot{m}\,(v_r - v_c) = \rho_1 v_r^2 - \rho_c v_c^2 = p_c - p_1 \quad , \tag{1.2}$$

$$e_c + \frac{p_c}{\rho_c} + \frac{1}{2} v_c^2 + q = e_1 + \frac{p_1}{\rho_1} + \frac{1}{2} v_r^2 \quad , \tag{1.3}$$

where

$$e_1 = \frac{1}{\gamma-1}\frac{p_1}{\rho_1},\quad q \equiv \frac{\Phi}{\dot{m}} - \frac{\epsilon_{ph}}{m_a},\quad v_c = -u_\phi,\quad v_r = v_1 - u_\phi, \qquad (1.4)$$

subscript c denotes condensate and subscript 1 quantities downstream from the discontinuity (ablation or vaporization front) in a laboratory frame of reference. v_r is the velocity relative to the discontinuity surface. The quantity q represents energy flux per unit mass and is thus a function of the ablation rate itself. At sufficiently large flux values the energy spent on phase transition may be neglected in the energy balance, i.e. $q \approx \Phi/\dot{m}$. The pressure in the condensed matter p_c was corrected by Gralnick [8] by the amount of the momentum flux carried by the incident plasma particles.

The system of equations (1.1) to (1.4) is supplemented by the Jouguet condition

$$v_r^2 = \gamma p_1/\rho_1. \qquad (1.5)$$

The state parameters of the condensed phase (ρ_c, p_c, e_c) are assumed to be known.

Equations (1.1) and (1.2) yield the well-known Rayleigh relation:

$$p_c - p_1 = \rho_c v_c^2 \,(\rho_1^{-1} - \rho_c^{-1}), \qquad (1.6)$$

whereas equ. (1.3) can be reduced, by means of equ. (1.6), to the Hugoniot equation:

$$e_c - e_1 + q = \frac{1}{2}(p_1 + p_c)\,(\rho_1^{-1} - \rho_c^{-1}). \qquad (1.7)$$

With the help of equs. (1.5), (1.6), (1.7), and the equation of state Gralnick arrived at the following quadratic relation:

$$\frac{\gamma+1}{\gamma-1}\left(\frac{v_r}{v_c}\right)^2 + 2\,\frac{\gamma+1}{\gamma}\left(\frac{v_r}{v_c}\right) - \frac{e_c + q - v_c^2/2}{v_c^2/2} = 0,$$

whose solution he gave for $\gamma = 5/3$ as

$$\epsilon \equiv v_r/v_c = 0.4 \pm \{\, 0.16 + 0.25\,[(e_c + q)/\tfrac{1}{2}u_\phi^2 - 1]\}^{1/2}.$$

Note that ϵ reduces to unity at zero heat flux only if $e_c/u_\phi^2 \to [\gamma(\gamma-1)]^{-1}$, i.e. if u_ϕ approaches the isentropic signal velocity of an ideal gas. Hence Gralnick implicitly applies the ideal gas state equation to the condensed phase as well. Note, furthermore, that in the above equation not only ϵ but also u_ϕ and q are as yet unknowns. At this point, Gralnick introduced two additional assumptions: (a) he replaced the unknown energy flux per unit mass by a given energy input per particle [8a]: $q = (1.5\,W_o - E_{H_2})/2\,m_D$, $W_o \approx 36$ eV, $E_{H_2} \approx 31.67$ eV, and $m_D \approx 3.35 \times 10^{-27}$ kgm; (b) he substituted for the ablation front velocity $u_\phi = -v_c$ the value obtained for a shperical pellet in a zeroth order approximation (see equ. (0.5)) by assuming Maxwellian electron energy distribution [8b]. With q and v_c known, v_r and the rest of the flow parameters can readily be found from the above set of equations. For an assumed set of reactor plasma conditions ($n = 10^{15}$ cm^{-3}, $T = 10^8$ °K, $\Phi \approx 4 \times 10^9$ W/cm^2) he obtained the following ablation parameters: $|u_\phi| = 1.3 \times 10^2$ m/s, $v_1 \approx 1.3 \times 10^4$ m/s, $T_1 \simeq 2.4 \times 10^4$ °K, and $\rho_1/\rho_c \approx 10^{-2}$.

Note, however, while the first of the above assumptions is permissible in a mathematical sense (it only decouples the ablation rate parameters from the actual reactor flux conditions), the second assumption makes the problem over-determined. Indeed, if the state parameters of the condensed phase are given, equs. (1.1) to (1.3) with equ. (1.5) are necessary and sufficient for unique determination of the four unknowns v_c, v_r, p_1, and ρ_1 (and of the associated quantities u_ϕ, v_1, $\dot{m}$, and e_1) in terms of the given energy flux Φ. Moreover, as shall be shown in the next section, the solution can be obtained in explicit form.

1.2 The Two-Phase Jouguet-Type Ablation Model

For the sake of simplicity, it shall be assumed that the equation of state of an ideal gas applies also to the condensed phase (the problem also being solvable without this assumption). Eliminating the pressures and internal energies from equ. (1.7) by means of equs. (1.4), (1.1), (1.5), and (1.6), we obtain

$$\left.\begin{aligned} &x^2 - 2x + 1 - 2\mu q/v_r^{\,2} = 0, \\ &\text{where} \quad x \equiv \rho_1/\rho_c = v_c/v_r \text{ and } \mu \equiv (\gamma-1)/\gamma+1). \end{aligned}\right\} \tag{1.8}$$

Introducing now the notation

$$\hat{v}^2 \equiv 2\mu q \approx 2\mu(\Phi/\dot{m} - \epsilon_{ph}/m_a) \approx 2\mu\Phi/\dot{m}, \tag{1.9}$$

the solution of (1.8) yields

$$\frac{\rho_1}{\rho_c} = \frac{v_c}{v_r} = 1 \pm \frac{\hat{v}}{v_r}, \tag{1.10}$$

$$-u_\phi = v_c = v_r \pm \hat{v}, \tag{1.11}$$

$$v_1 = \mp \hat{v}. \tag{1.12}$$

A combination of equations (1.2), (1.5), (1.10), and (1.11) yields a quadratic equation relating v_r and $\hat{v}$:

$$v_r^2 \mp (\gamma-1)\,\hat{v}\,v_r - (c_c^2 + \gamma\hat{v}^2) = 0, \text{ i.e.} \tag{1.13a}$$

$$v_r = \tfrac{1}{2}(\gamma+1)[\pm\mu \pm \sqrt{1+\eta}\,]\hat{v} \tag{1.13b}$$

where

$$\eta \equiv \left(\frac{2}{\gamma+1}\right)^2 \left(\frac{c_c}{\hat{v}}\right)^2, \quad \text{and } c_c^2 \equiv \gamma p_c/\rho_c. \tag{1.14}$$

The first double sign in equ. (1.13b) originates from the solution of the quadratic equation (1.8), whereas the second one is from the solution of equ. (1.13a). As shall be seen, the selection of the proper sign combination is unique.
A second relation between v_r and $\hat{v}$ is obtained by substituting equ. (1.11) in equ. (1.9):

$$\hat{v}^2 = \frac{2\,\mu\,\Phi}{\rho_c\,(v_r \mp \hat{v})}.$$

Expressing v_r from this equation and substituting it in equ. (13a), we arrive at an explicit expression for $\hat{v}$:

$$y^4 \pm Ay^3 - 1 = 0, \quad \text{or} \quad y^3(y \pm A) = 1, \text{ where} \tag{1.15}$$

$$y \equiv \hat{v}/\hat{v}_c, \; \hat{v}_c \equiv \left(\frac{2\mu\Phi}{\rho_c c_c}\right)^{1/2}, \text{ and } A \equiv (\gamma+1)\hat{v}_c/c_c.$$

Note that the solution of equ. (1.15) may be positive or negative. Note, furthermore, that replacing y in (1.15) by -y only reverses the signs of the second term. Because of this symmetry property it is sufficient to consider only the positive solutions ($\hat{v} > 0$) of equ. (1.15). Since, by definition, $v_r > 0$ and $\sqrt{1+\eta} > \mu$ ($\gamma = 5/3$), we may rewrite equ. (1.13b) in its final form:

$$v_r = \frac{1}{2}(\gamma+1)(\sqrt{1+\eta} \pm \mu)\hat{v}\,; \quad \hat{v} > 0. \tag{1.13c}$$

We may now identify the two branches corresponding to the positive and negative signs in equs. (1.13c) or (1.15). As can be seen from equs. (1.10) and (1.12), the positive branch corresponds to compression: the compressed matter follows the propagating ablation front. This is a detonation-wave-like solution. The negative branch corresponds to expansion: the flow in this case is directed away from the discontinuity surface. This is a slow-burning-type subsonic flow solution.

Let us now consider the domain of y variations corresponding to the positive and negative signs in equ. (1.15). Since only positive $\hat{v}$ values are considered, as can readily be seen,

(a) positive branch: $1 \leq y \leq A^{-1/3}$; $0 \leq \hat{v}/c_c \leq \left(\frac{2\mu}{\gamma+1}\Phi^*\right)^{1/3}$,

(b) negative branch: $1 \leq y \leq A$; $0 \leq \hat{v}/c_c \leq 2(\gamma-1)\phi^*$, (1.14)

where $\Phi^* \equiv \Phi/\rho_c c_c^3$ (1.15)

is the dimensionless energy flux. The upper and lower limits correspond to $\Phi^* >> 1$ and $\Phi^* << 1$, respectively.

Assuming $\Phi^* >> 1$, which is certainly the case under reactor-like plasma conditions, and taking the values of $\hat{v}$ given by the upper limits of equs. (1.14), explicit expressions can be obtained for all plasma parameters both for the detonation-like and the slow burning-type solutions. The corresponding expressions are given in the first two columns of Table 1. All quantities denoted by asterisks are nondimensionalized by means of the condensed state parameters ($\rho_c \approx 167$ kgm/m^3, $T_c \approx 10\ ^oK$, $c_c \approx 262$ m/s).

For moderate and small values of Φ^*, $\hat{v}$ is determined by solving equ. (1.15) for $y = \hat{v}/\hat{v}_c$ (an iterative solution is straightforward). Ablation product parameters calculated by this method are shown in Fig. 2 as functions of the energy flux ϕ both for the detonation-like and the slow-burning wave solutions. Note that with $\phi \to o$ $u_\phi \to c_c$ (see (equ. 1.13a with $\hat{v} \to o$) and thus the dimensionless mass flow $\dot{m}^* = |u_\phi^*|$ defined in accordance with equ. (1.1) approaches to unity instead of zero. For this reason, at low energy fluxes it is advisable to use the product $\rho_1 v_1$ for determining the ablation rate. As can be seen from Fig. 2, $\rho_1 v_1 \to |u\phi|\, \rho_c$ at $\phi \gtrsim 10^{10}$ W/m^2. The results corresponding to $\Phi \approx 4 \times 10^{14}$ W/m^2 are quite different from those calculated by Gralnick[8].

Note the basically different functional dependences on Φ^* in the two cases considered (detonation-like, slow burning-type solutions). While the detonation-like solution predicts increasing mass flow and increasing ablation rate at higher energy fluxes, in the case of an expansion-type

solution the ablation front velocity and the mass flow decrease with increasing energy flux (in contrast to Gralnick's model, in which $\dot{m}^* \propto \Phi^*$ was assumed a priori, and, as a result of overdetermining the problem, an expansion solution ($\rho_1/\rho_c \ll 1$) was found). This second case in fact corresponds to heat being added to an already choked flow (a consequence of the Jouguet condition), which, as is well known in gas dynamics, causes a reduction of the flow throughput.

Summarizing the results of this two-phase Jouguet flow approximation one sees that two types of solutions are possible: one corresponds to compression and reversed flow behind the ablation front, the other to expansion and outwardly directed flow. Intuitively, one would not expect reversed flows and vapor densities higher than solid phase density in ordinary ablation processes. Besides, the incident radiation in this case would be intercepted by the shocked material; hence the basic assumption of the model (energy deposition at the discontinuity surface) would be violated. This model can thus probably be omitted from further considerations. On the other hand, the $\dot{m} \propto \Phi^{-1}$ proportionality characterizing the expansion solution cannot be considered as physically realistic either. Hence the two-phase Jonguet model is not generally applicable even if it is posed and solved correctly. The defficiency of this model is due to neglecting an essential physical phenomenon: the intense energy deposition at the surface discontinuity inevitably leads to the formation of a shock wave which penetrates the condensed phase preceeding the ablation wave. Part of the energy flux transmitted to the medium is dissipated in the shock wave and the ablation wave propagates in a shock-heated medium. It is thus necessary to

TABLE 1. TWO-PHASE MODEL SOLUTIONS, LARGE ENERGY FLUX LIMIT

	DETONATION WAVE-LIKE	SLOW BURNING TYPE	SIMPLE SHOCK SOLUTION
v_1^*	$-\left(\frac{2\mu}{\gamma+1}\right)^{1/3}\Phi^{*1/3}$	$2(\gamma-1)\Phi^*$	$-\left(\frac{a-1}{a}\right)^{2/3}\phi^{*1/3}$
η	$\left(\frac{4}{\gamma^2-1}\right)^{2/3}\Phi^{*-2/3}$	$\frac{1}{(\gamma^2-1)^2}\Phi^{*-2}$	-
v_r^*	$\gamma\left(\frac{2\mu}{\gamma+1}\right)^{1/3}\Phi^{*1/3}$	$2(\gamma-1)\Phi^*$	$\frac{1}{a}\left(\frac{a}{a-1}\right)^{1/3}\Phi^{*1/3}$
$-u_\phi^*$, v_c^*, $\dot{m}^*$	$[2(\gamma^2-1)]^{1/3}\Phi^{*1/3}$	$\frac{1}{2(\gamma^2-1)}\Phi^{*-1}$	$\left(\frac{a}{a-1}\right)^{1/3}\Phi^{*1/3}$
ρ_1^*	$\frac{\gamma+1}{\gamma}$	$\frac{1}{4}\frac{\gamma+1}{(\gamma^2-1)^2}\Phi^{*-2}$	$a = a_{max}(\phi^*)$
p_1^*	$\gamma\left[4\frac{(\gamma-1)^2}{\gamma+1}\right]^{1/3}\Phi^{*2/3}$	$\frac{1}{\gamma+1}$	$\frac{\gamma+1}{2}\frac{a-\mu}{a^{1/3}(a-1)^{2/3}}\phi^{*2/3}$
e_1^*	$\gamma^2\left(\frac{2\mu}{\gamma+1}\right)^{2/3}\Phi^{*2/3}$	$4(\gamma-1)^2\Phi^{*2}$	$\frac{\gamma+1}{2}\frac{a-\mu}{a^{4/3}(a-1)^{2/3}}\phi^{*2/3}$

consider a model consisting of at least three phases: the undistrubed condensed phase, the shocked phase, and the ablated material.

1.3 Three-Phase Jouguet-Type Ablation Model

The system considered is shown in Fig. 3 in a laboratory frame of reference. The ablation wave moving to the left with a velocity u_ϕ is preceded by a shock wave penetrating the undisturbed condensed phase with a velocity u_s. The density is assumed to decrease across the ablation front, i.e. the expansion-type solution is assumed to apply to the second discontinuity surface. The conservation equations applied to the dicontinuity surfaces and, written in the respective relative reference frames, are as follows:

$$\dot{m}_s = -\rho_c u_s = \rho_s (v_s - u_s), \tag{1.16}$$

$$\rho_s (v_s - u_s)^2 - \rho_c u_s^2 = p_c - p_s, \tag{1.17}$$

$$e_c + \frac{p_c}{\rho_c} + \frac{1}{2}u_s^2 = e_s + \frac{p_s}{\rho_s} + \frac{1}{2}(v_s - u_s)^2, \tag{1.18}$$

$$\dot{m}_\phi = \rho_s (v_s - u_\phi) = \rho_1 (v_1 - u_\phi), \tag{1.19}$$

$$\rho_1 (v_1 - u_\phi)^2 - \rho_s (v_s - u_\phi)^2 = p_s - p_1, \tag{1.20}$$

$$e_s + \frac{p_s}{\rho_s} + \frac{1}{2}(v_s - u_\phi)^2 + q = e_1 + \frac{p_1}{\rho_1} + \frac{1}{2}(v_1 - u_\phi)^2, \tag{1.21}$$

where $e = \frac{1}{\gamma - 1}\frac{p}{\rho}$, and $q \approx \frac{\Phi}{\dot{m}_\phi}$.

As before, the equations are supplemented by the Jouguet condition:

$$(v_1 - u_\phi)^2 = \gamma \frac{p_1}{\rho_1}. \tag{1.22}$$

A unique solution of the above system of equations requires, in addition to the Jouguet condition, specification of still another constraint (unkown: u_s, u_ϕ, v_s, v_1, p_s, p_1, ρ_s, and ρ_1). There exist some obvious physical arguments which could lead to an additional condition but, unfortunately, none of these yield a single-valued explicit constraint of the type of equ. (1.22). For example, if steady-state conditions are to prevail, the stagnation pressure downstream from the ablation wave may not be less than the ambient pressure. This condition defines a whole range of admissible total pressure values.

Instead of choosing any particular and, to some extent, artificial constraint at this point, we shall first obtain a series of solutions with one of the flow variables as a free parameter. Analysis of the solutions thus obtained may then define the region of physically possible plasma parameter values.

Note that equs. (1.16) to (1.18) are the conventional shock wave equations and their solution is unique if one of the shock parameters is given. We shall thus proceed as follows: prescribing a compression ratio

$$a \equiv \rho_s/\rho_c = \rho_s^* \tag{1.23}$$

we compute the state variables behind the shock wave by means of the Rankine-Hugoniot relations:

$$\left.\begin{aligned} p_s^* &= \frac{a-\mu}{1-a\mu}\,; \quad u_s^* = \dot{m}_s^* = -\left(\frac{2}{\gamma+1}\,\frac{a}{1-\mu a}\right)^{1/2} \\ v_s^* &= \left(1-\frac{1}{a}\right)u_s^*\,, \text{ and } e_s^* = c_s^{*2} = \frac{1-\mu/a}{1-\mu a}\,. \end{aligned}\right\} \tag{1.24}$$

The energy dissipated in the shock wave is given by the change of the stagnation temperature of the gas in the laboratory frame of reference:

$$\Phi_s = \dot{m}_s\left[\frac{1}{2}v_s^2 + \frac{\gamma}{\gamma-1}\left(\frac{p_s}{\rho_s} - \frac{p_c}{\rho_c}\right)\right]. \tag{1.25}$$

The energy flux affecting the gas at the ablation front is the difference between the total energy flux deposited in the ablation wave Φ and the energy flux expended on shock-heating the condensed matter:

$$\Phi_{eff} = \Phi - \Phi_s. \tag{1.26}$$

Hence defining

$$y \equiv \frac{\hat{v}}{\hat{v}_s}\,, \quad A \equiv (\gamma+1)\,\frac{\hat{v}_s}{c_c}, \quad \text{and } \hat{v}_s \equiv \left(\frac{2\mu\Phi_{eff}}{\rho_s c_s}\right)^{1/2}, \tag{1.27}$$

all flow parameters can readily be computed by finding $\hat{v}$ from equ. (15) and following the procedure outlined avbove.

The value of "a" can be varied between 1 and $a_{max} = a_{max}(\Phi_s)$, where the lower limit corresponds to vanishing shock wave strength ($\Phi_{eff} \approx \Phi$, $\Phi_s \to 0$), and the upper limit corresponds to the case where all energy is dissipated in the shock wave ($\Phi_s \approx \Phi$, $\Phi_{eff} \to 0$). For the case $a \to 1$ the slow burning-type solution displayed in Table 1 is applicalbe, whereas the second case ($a \to a_{max}$) corresponds to a two-phase shock model, without the Jouguet condition applied. An analytic solution with $\Phi_s = \Phi$ as given parameter can be obtained for this limiting case as well. Indeed, expressing Φ_s ,defined by equ. (1.25), in terms of the compression ratio a, we obtain, with the help of the Rankine-Hugoniot relations,

$$\Phi_s^* = \frac{\Phi_s}{\rho_c c_c^3} = \left(\frac{2}{\gamma-1}\right)^{3/2} \frac{a^{1/2}(a-1)}{(1-\mu a)^{3/2}} \quad . \tag{1.28}$$

This is the equation that defines $a = a_{max}$ in terms of a given Φ_s^* value. The value of "a" can readily be found from equ. (1.28) by iterative means. Furthermore, assuming $a = a_{max}$, the shocked flow parameters can be expressed as functions of the dimensionless energy flux Φ_s^* by means of equ. (1.28). The results are given in the last column of Table 1 (see also the corresponding curves in Fig. 2). As can be seen, the functional dependence is the same, as in the case of the detonation-wave-like solution, only the numerical factors being different. This difference is due to the absence of the Jouguet condition in the ordinary shock wave solution. The quantity "a", of course, is itself a function of Φ_s^*, but its variation may be neglected if $\Phi_s \gtrsim 10^{13}$ W/m^2 ($a_{max} \to 4$).

Varying the value of a between 1 and a_{max}, sets of solutions to equs. (1.16) to (1.22) can be obtained for any given Φ value. Typical reduced flow parameter variations are shown in Fig. 4 as functions of a for $\phi = 10^{11}$ w/m^2. In the same figure, the ratio of the energy flux dissipated in the shock wave and the total energy flux absorbed is also shown.

The existence of several characteristic flow regions can readily be observed in Fig. 4. For $a \gtrsim 3.13$ one has $u_\phi^* > u_s^*$ and thus no steady state exists with two discontinuity surfaces. In the region $a \gtrsim 3.1$ the value of ρ_1^* becomes greater than unity. As has been discussed above, this situation is also inadmissible under steady-state conditions. Finally, if $a \gtrsim 3.01$, $v_1 > 0$, i.e. the ablated material streams towards the condensed phase as in the case of detonation and shock waves. This case, too, is very unlikely to occur under normal ablation conditions. The same characteristic parameter regions are found at other incident flux intensities at well. Moreover, at high flux intensities still another constraint may be defined which imposes a lower limit on the value a: the temperature T_1 should not exceed the ambient plasma temperature.

We may consider the $v_1 \to 0$ case as the upper limit for ablation rates and the associated plasma parameters. The reduced mass flow rate $\rho_s^* u_\phi^*$ and the temperature T_1^* corresponding to this upper limit are plotted in Fig. 5 as functions of the incident energy flux Φ. For the sake of comparison, ablation rate and temperature values corresponding to the average compression ratio within the inverval $1 \leq a \leq a(v_1 = 0)$, $\langle \rho_1^* v_1^* \rangle$ and $\langle T_1^* \rangle$, respectively, are also shown in this figure. As can be seen, at high flux intensities the value of $\langle T_1^* \rangle$ approaches to the limit

represented by the abmient plasma temperature. Realistic ablation parameter values should lie between the respective limit curves shown in Fig. 5.

The ablation rates obtained from the three-phase Jouguet model without shielding effects present are extremely high. The pellet injection velocities associated with these ablation rates under reactor conditions are well over 10^4 m/s.

2. ABLATION IN THE PRESENCE OF MAGNETIC FIELD

2.1 Rose's Balloon Model

Rose [5] assumed that the ablated material ionizes instantaneously at the pellet surface and expands by blowing a diamagnetic balloon around the pellet. The main feature of this model is the reduced heat flux to the pellet: assuming that the particles are confined to magnetic surfaces, energy is transferred to the ablated material only by those gyrating particles whose orbits dip into the sides of the balloon as they travel along it. Thus the balloon model consists of three regions (spherically symmetric geometry): (a) the cold pellet of radius r_p, (b) the fully ionized diamagnetic balloon of radius r_1 surrounding the pellet and consisting of a plasma of temperature T_1, density n_1, $\beta_1 = 1$ ($B_1 = 0$), (c) the unperturbed background plasma with n_o, T_o, B_o, where $p_o + B_o^2/2\mu_o = B_{vac}^2/2\mu_o$. The state parameters of the unperturbed plasma are known. It is assumed that $n_e = n_i$ and $T_e = T_i$ in all regions. The ablation products can only escape along the magnetic field lines, and the outflow velocity is assumed to be the local sonic velocity (flow area $\approx \pi r_1^2$). Rose described this

model in a magnetostatic approximation by means of the following equations:

Particle continuity: $\pi r_1^2 n_1 v_s = G,$ (2.1)

Pressure balance: $2n_1 kT_1 = B_{vac}^2/2\mu_o,$ (2.2)

Energy balance at $r = r_p$: $a_p F_1 = G\,\epsilon_i$ (2.3)

Energy balance at $r = r_1$: $a_1 F_o = G(\epsilon_i + 3\,k\,T_1),$ (2.4)

where $G(sec^{-1})$ is the particle ablation (ionization) rate, $F_1 = 0.5\, n_1 v_{e1th} kT_1$ and $F_o = 0.5\, n_o v_{eoth}\, kT$ are energy fluxes (correspinding to Maxwellian distributions) at the respective surfaces, $a_p = 4\pi r_p^2$, $a_1 = \pi[(r_1+r_c)^2 - r_1^2] \approx 2\pi r_1 r_c$, $r_c = mv/eB << r_1$ is the gyro-radius, and $v_s = (2T_i/m_i)^{1/2}$. Since $r_{ci} v_{ith} T_i = r_{ce} v_{eth} T_e$, only one species of particles is considered as energy carriers and the energy spent on heating the vaporized gas is neglected. The ablation kinetics (ablation or shock wave propogation, etc.) is not considered in this approximation. The above set of equations is sufficient for unique determination of the four unknowns G, r_1, n_1, and T_1:

$$G = \frac{\pi r_p^2}{\epsilon_i} \frac{B_{vac}}{2\mu_o} \left(\frac{8kT_1}{\pi m_e}\right)^{1/2} \quad \text{(equs. 2.2 and 2.3),} \tag{2.5}$$

$$\frac{r_1}{r_p} = \left(\frac{32}{\pi} \frac{m_a}{m_e}\right)^{1/4} \left(\frac{kT_1}{\epsilon_i}\right)^{1/2} \quad \text{(equs. 2.1 and 2.3),} \tag{2.6}$$

$$n_1 = \frac{B_{vac}^2}{4\mu_o kT_1} \quad \text{(equ. 2.1), and} \tag{2.7}$$

$$\frac{kT_1}{\epsilon_i} = \frac{1}{3}\left[\left(\frac{n_o kT_o}{B_{vac}^2/2\mu_o}\right)\left(\frac{32}{\pi}\frac{m_e}{m_a}\right)^{1/4} \left(\frac{r_{ci}}{r_p}\right) \left(\frac{kT_o}{\epsilon_i}\right)^{1/2} - 1\right]. \tag{2.8}$$

A thorough analysis of Rose's solution was given by Chang[7]. He showed that the plasma temperatures obtained from this solution are much too low ($T_1 \approx 1$ eV under reactor plasma conditions) to justify the assumption of a fully ionized diamagnetic balloon around the pellet. Chang also showed that, in the framework of this model, physically possible solutions ($T_1 > 0$) are only possible for certain pellet size and magnetic field strength combinations.

2.2 Chang's Magnetic Nozzle Model

Since the blanket surrounding the ablating pellet is not likely to be fully ionized, Chang[7] allowed for the presence of magnetic field in the blanket by prescribing the ratio

$$\epsilon \equiv B_1^2/2\mu_o p_1 \quad , \tag{2.9}$$

where subcript 1 denotes parameter values around the pellet and at the entrance section of the "magnetic nozzle". His model is described by means of the following equations (see also Fig.6):

$$\rho_{av} = \rho_1 a_1 v_1 \quad , \tag{2.10}$$

$$p/\rho^\gamma = p_1/\rho_1^\gamma \quad , \tag{2.11}$$

$$\rho v^2 - \rho_1 v_1^2 = p_1 - p \quad , \tag{2.12}$$

$$p + B^2/2\mu_o = \text{const} = p_o + B_o^2/2\mu_o = B_{vac}^2/2\mu_o \quad , \tag{2.13}$$

$$aB = a_1 B_1 \quad , \tag{2.14}$$

where a is the stream tube cross-section: $a = \pi r^2$. Equation (2.14) implies that the stream tubes are identical with flux tubes, i.e. the plasma is only allowed to move along the magnetic field lines. Hence the ablation products stream away from the pellet as if they were enclosed by a (flexible) nozzle. The pressure variation is coupled to the magnetic field strength variation along the nozzle by means of equ. (2.13). Chang has assumed that the flow becomes sonic at the nozzle throat:

$$v_* = (\gamma p_* / \varrho_*)^{1/2}, \tag{2.15}$$

and that the throat area is equal to the pellet cross-section:

$$a_* = a_p \; ; \quad r_* = r_p. \tag{2.16}$$

He further assumed that the throat pressure is given by the surrounding (known) plasma pressure:

$$p_* = p_o \; , B_* = B_o \; , \tag{2.17}$$

i.e. undisturbed background plasma conditions prevail at the throat of the nozzle. Similarly to Rose's approach, the ablation kinetics is neglected also in this approximation; the ablation rate G is assumed to be given by

$$G = \pi r_p^2 \, n_1 \, v_{1th} \, kT_1/\epsilon_i. \tag{2.18}$$

As can be seen, the first three of the above equations correspond to isentropic nozzle flow, and hence, for stations between a_1 and a_*, the relation known from ideal gas dynamics apply (equ. 4.8 of Chang[7]):

$$\left(\frac{a_*}{a_1}\right)^2 = \left(\frac{r_p}{r_1}\right)^4 = \frac{\gamma+1}{\gamma-1}\left[1-\frac{2}{\gamma+1}\left(\frac{p_1}{p_o}\right)^{\frac{\gamma-1}{\gamma}}\right]\left(\frac{p_1}{p_o}\right)^{\frac{2}{\gamma}}. \qquad (2.19)$$

Considering equs. (2.14) and (2.16) together, one notices that only those magnetic flux surfaces that were initially embedded in the cold pellet remain trapped in the ablation products. The flux tube, which was originally attached to the cold pellet surface, forms the boundary of the magnetic nozzle at later times, i.e. no field or particle diffusion takes place across this boundary. Hence the external magnetic field does not really penetrate the ablation products and the model is in this respect not different from Rose's diamagnetic balloon model.

Note, furthermore, that it follows from equs. (2.9) and (2.13) that

$$p_1 = \frac{B_{vac}^2/2\mu_o}{1+\epsilon}, \text{ and } \left(\frac{B_1}{B_{vac}}\right)^2 = \frac{\epsilon}{\epsilon+1}. \qquad (2.20)$$

Furthermore, equs. (2.14), (2.16), and (2.17) yield

$$\left(\frac{r_1}{r_p}\right)^4 = (1-\beta)\frac{\epsilon+1}{\epsilon}, \text{ where } \beta \equiv \frac{p_o}{B_{vac}^2/2\mu_o}$$

is a given parameter. Since

$$\frac{p_1}{p_o} = \frac{B_{vac}^2/2\mu_o}{1+\epsilon}\,\frac{2\mu_o}{\beta\, B_{vac}^2} = \frac{1}{\beta(1+\epsilon)},$$

we obtain

$$\left(\frac{r_1}{r_p}\right)^4 = \frac{1-\beta}{1-(p_1/p_o)\beta} \quad ; \qquad (2.21)$$

which is a second relation between (r_1/r_p) and (p_1/p_o) incompatible with that obtained from ideal gas dynamic considerations (equ. 2.19). Hence, the system of equations treated by Chang is also overdetermined.

There is no simple way to modify this model. To remove one of the constraints used, one would necessarily have to change a number of other assumptions as well. For example, if we remove the $r_* = r_p$ constraint, the pressure could be computed from equ.(2.20). However, $r_* \neq r_p$ is equivalent to allowing for field penetration and thus equs. (2.14) and (2.17) would have to be modified as well.

Since field penetration is a diffusion process, any steady-state approximation allowing for non-vanishing magnetic fields in the ablation plasma should include some assumption regarding the inward diffusion of the magnetic field and the outward motion of the ablated and ionized matter.

2.3 Magnetic diffusion model

The model considered here can be described as follows: The pellet is initially in direct contact with the surrounding plasma and thus the ablated particles are ionized within a time $\Delta t_i = \Delta t_i\ (n_{eo}, T_{eo})$, where subscript "o" denotes the

surrounding plasma ($n_{eo} = n_o$, $T_{eo} = T_o$). Considering collisional ionization, this time is much shorter than the ablation time in all cases of practical interest. As time goes on, the ablated particles form a blanket around the pellet, whose temperature is different from the unperturbed plasma temperature: $T_1 < T_o$. The ionization front moves some distance away from the pellet surface ($r_1 > r_p$). Some of the electrons in the blanket recombine,and, since the characteristic recombination times are also much shorter than the ablation times (owing to the high densities), the electron density in the blanket n_{e1} may be approximated to a fairly good degree of accuracy by the equilibrium (Saha) density value corresponding to the temperature T_1. The particles ablated leave the pellet with a random velocity whose magnitude lies in the range given by equs. (0.7), and are ionized after a time $\Delta t_i = \Delta t_i\ (n_{e1}, T_1)$, where subscript "1" denotes parameter values in the blanket around the pellet. The ionization front while moving outward displaces the magnetic flux lines. If field diffusion could be neglected, the magnetic flux originally imbedded in the pellet would be distributed over the blanket of radius r_1. However, as will be shown, the penetration depth of the magnetic field Δl is comparable in some cases to the blanket radius or is even larger. The penetration depth is given by

$$\Delta l = (\Delta\tau/\sigma_1\mu_o)^{1/2}.$$

The field penetration is complete if the field diffusion velocity is greater than or equal to the outward directed flow velocity, i.e. if

$$v_D = \frac{\Delta \ell}{\Delta \tau} = (\sigma_1 \mu_o \Delta \tau)^{-1/2} > v_1 = \frac{\Delta r}{\Delta \tau};\ \Delta r = r_1 - r_p,$$

i.e. if

$$Rm \equiv \sigma_1 \mu_o v_1 \Delta r < 1, \qquad (2.22)$$

where Rm is the magnetic Reynolds number based on the blanket parameters. Thus the Rm = 1 condition represents the limit between magenitzed and diamagnetic ablation plasmas.

It is assumed that the electrons heating the pellet can only move along the magnetic flux lines. Energy is thus transported only along those flux lines which either pierce the blanket or are at a distance from it not larger than the electron gyro-radius. The effective area exposed to the thermal flux $\Phi_o = 0.5\, n_o v_{eo} kT_o$ is thus given by

$$a_1 = 2\pi \{r_p^2 + [\, r_1^2 - (r_1 - \Delta \ell)^2] + [(r_1 + r_{ec})^2 - r_1^2]\},$$

where the first and second terms of the r.h.s. account for the magnetic flux lines that were originally imbedded in the pellet and those diffused into the blanket, while the third term accounts for the gyrating electrons, whose trajectory dips into the sides of the blanket. The energy carried by the gyrating ions is accounted for simply by doubling the corresponding electron flux term. As can readily be seen, for magnetic field strengths of practical interest ($B \gtrsim 3$ T), this contribution is altogether negligible relative to the fluxes corresponding to the first two terms. There is of course a limit on a_1 : $a_1 \lesssim 2\pi r_1^2$.

A quasi-steady approximation is used, the time--dependent build-up of the blanket around the pellet not being considered here. The shock kinetics discussed in the previous sections as well as the phenomena associated with the finite penetration depths of the incident particles in the blanket are also left out of consideration. It is assumed that the energy flux incident on the pellet surface causes only vaporization, and that the radial velocity component of the vaporized particles v_{vap} can be approximated by the sonic velocity at the pellet temperature. The major part of the energy is transferred to the particles at the blanket-plasma interface. It is assumed, furthermore, that the vapor velocity does not change appreciably over the ionization length Δr. The motion remains spherically symmetric up to the ionization radius r_1, and the charged particles then lose their radial momentum and leave the blanket region along the magnetic flux lines.

The system of equations defining the model can thus be written in the following form:

$$2\pi r_1^2 \eta \Phi_o = G(\tfrac{1}{2} m_a v_1^2 + \tfrac{3}{2} kT_1) + G_e\ (\varepsilon i + \tfrac{3}{2} kT_1), \tag{2.23}$$

$$4\pi r_p^2 \Phi_1 = G\, \epsilon_{vap}, \tag{2.24}$$

$$r_1 - r_p = \Delta t_i v_{vap};\ \Delta t_i = (n_{e1} S_{c1})^{-1};\ S_{c1} = S_c(n_{e1}, T_1) \tag{2.25}$$

where

$$G = G_a + G_e,\ G_a = 4\pi r_1^2 n_a v_1,\ G_e = 2\pi r_1^2 n_e v_1,$$

$\eta = \min(\eta_o, 1)$, $\Delta\ell = \Delta r/Rm_1^{1/2} \approx r_1/Rm_1^{1/2}$, $Rm_1 = \sigma_1 \mu o v_1 r_1$, and

$$\eta_o = (r_p/r_1)^2 + Rm_1^{-1/2}\,(2-Rm_1^{-1/2}) + 2\,(r_{ec}/r_1)\,(2 + r_{ec}/r_1).$$

In the present estimates, the ionization coefficient values tabulated by Düchs[9] on the basis of the analysis of Bates, Kingston, and McWhirter[10] have been used. The above equations are supplemented by the Saha relation

$$n_{e1} = \alpha n_1,\ \alpha^2/(\alpha-1) = f_s/n_1,$$

where $n_1 = n_a + n_e$, and $f_s = \text{const.}\ T_1^{3/2} \exp(-\epsilon_i/kT_1)$ (2.26)

The energy flux ϕ is defined by equ. (0.3). We thus have four equations (2.23) to (2.26) with five unknowns: n_1, n_{e1}, T_1, v_1, and r_1.

Sonic approximation. To make the above system of equations closed, we shall assume, as Rose[5] and Chang[7] did, that the ablation plasma leaves the blanket with sonic velocity:

$$v_1^2 = c_1^2 = \gamma p_1/\rho_1;\ p_1 = n_a kT_1 + 2\, n_{e1} kT_1;\ \rho_1 = n_1 m_a. \quad (2.27)$$

With this assumption the above set of equations reduces to (MKS system):

$$\eta\phi_o = n_1 c_1 kT_1\,\{(1-\alpha/2)\,[\gamma(1+\alpha) + 3] + \alpha\,(\epsilon_i/kT_1 + 3/2)\}, \quad (2.28)$$

$$\frac{r_1}{r_p} = \left(\frac{74.92}{(\alpha+1)^{1/2}}\,\frac{\alpha}{2-\alpha}\,\frac{kT_1}{\epsilon_{vap}}\right)^{1/2}, \quad (2.29)$$

$$r_1 - r_p = v_{vap}\Delta t_i\ , \quad (2.30)$$

$$n_{e1} = n_e(n_1,T_1)_{Saha},\ c_1 = [\gamma(1+\alpha)\ kT_1/m_a]^{1/2} \qquad (2.31)$$

which can be solved iteratively for any given values of ϕ_o, r_p, and v_{vap} ($v_{vap} \approx (\gamma kT_c/m_a)^{1/2} \approx 262$ m/s). Results calculated on the basis of this approximation are displayed in Table 2 for ϕ_o flux values ranging from present low-temperature boundary layer ablation experiments up to future reactor conditions. A discussion of the results follows below.

Approximation with transverse momentum balance. As is known from laser-plasma calculations[11, 12], the assumption of sonic flow is a rather crude approximation for spherical flows with energy influx. It is thus of interest to check in what way and to what extent the ablation parameters change if the sonic constraint is removed. Since the velocity v_1 is now an unknown quantity, an additional condition is introduced in the form of the transverse momentum balance:

$$(p + \rho v^2 + B^2/2\mu_o)_{r \lesssim r_1} = p_o + B_o^2/2\ \mu_o = B_{vac}^2/2\mu_o. \qquad (2.32)$$

Since the magnetic field penetrates into the blanket to a depth $\Delta\ell$ and the ionization radius r_1 is thus located in the region of the surrounding magnetic field, there is no field discontinuity at $r = r_1$ and equ. (2.32) reduces to

$$(1-\alpha)\rho_1 v_1^2 + (1+\alpha) n_1 kT_1 = 2n_o kT_o. \qquad (2.33)$$

For checking the effect of the magnetic pressure on the ablation parameters, some calculations were performed also by retaining the $B^2/2\mu_o$ term in the above equation and assuming that

$$\pi r_p^2 B_o = \pi (r_1 - \Delta\ell)^2 B_1, \qquad (2.34)$$

which is an additional equation defining $B_1 = B(r \lesssim r_1)$. In the momentum balance approximation equ. (2.28) is replaced by

$$\eta\phi_o = n_1 c_1 kT_1 M_1 \{(1-\alpha/2)[(1+\alpha)\gamma M_1^2 + 3] + \alpha(\epsilon_i/kT_1 + 3/2)\} \qquad (2.35)$$

and is supplemented by an equation that can be obtained from equ. (2.33):

$$(1+\alpha)\,[1 + (1-\alpha)\gamma M_1^2]\, n_1 kT_1 = 2 n_o kT_o. \qquad (2.36)$$

The system becomes somehwat more complicated if equ. (2.33) is replaced by equs. (2.32) and (2.34).

An iterative solution to the above system of equations is somewhat tedious, but possible. Results based on the approximation with equ. (2.33) (or eq. 2.36) are displayed in Table 3.

Discussion of the results.

The parameters r_1, n_1, T_1, $M_1 = v_1/c_1$, and the ablation rate G are displayed in Tables 2 and 3 as functions of the input parameters $\phi_o(n_o, T_o)$ and r_p. The last two rows in both tables correspond to two different pellet sizes at the same flux value (reactor plasma conditions). The ablation time $\tau = N_p/G$ is also shown in Table 3.

The results corresponding to the two different approximations display a common characteristic: as the flux intensitiy ϕ_o increases, the blanket radius r_1 decreases, but, at the same time, the blanket density n_1 increases, and so the blanket temperature T_1 remains practically constant (of the order of 1 eV), over 5 orders of magnitude of ϕ_o-variation. Hence the

TABLE 2 MAGNETIC DIFFUSION MODEL, SONIC APPROXIMATION ($M_1 = 1$)

$\phi_o (\frac{W}{m^2})$	$n_o (cm^{-3})$	T_o(eV)	r_p(mm)	r_1(mm)	$n_1 (cm^{-3})$	T_1(eV)	$G(s^{-1})$
2×10^7	1.2×10^{13}	1.0×10	0.31	43.8	2.0×10^{14}	1.80	4.17×10^{22}
10^9	2.0×10^{13}	9.7×10	0.60	16.1	1.0×10^{17}	1.05	3.07×10^{24}
$\approx 10^{11}$	2.0×10^{13}	2.0×10^3	0.61	3.15	1.4×10^{19}	0.99	2.11×10^{25}
10^{13}	1.0×10^{14}	1.5×10^4	0.60	1.00	1.6×10^{21}	0.97	1.76×10^{26}
10^{13}	1.0×10^{14}	1.5×10^4	5.10	6.35	1.7×10^{21}	0.92	7.45×10^{27}

TABLE 3 MAGNETIC DIFFUSION MODEL, MOMENTUM BALANCE [a)]

$\phi_o (\frac{W}{m^2})$	r_p(mm)	r_1(mm)	$n_1 (cm^{-3})$	T_1(eV)	M_1	$G(s^{-1})$	τ(μs)
2×10^7	0.33	42.8	4.8×10^{14}	2.50	1.70	1.75×10^{22}	433
10^9	0.60	36.8	9.7×10^{14}	1.38	3.90	4.85×10^{23}	93
10^{11}	0.59	17.5	1.7×10^{15}	1.35	15.3	7.70×10^{23}	56
10^{13}	0.61	9.5	3.3×10^{15}	1.36	55.4	1.50×10^{24}	31
10^{13}	5.15	6.9	1.7×10^{15}	1.20	54.3	4.25×10^{25}	678

a) The n_o and T_o values corresponding to a particular ϕ_o are the same as in Table 2.

ablation process seems to be self-regulating: the constant (flux-independent) blanket temperature provides an effective shielding also at high flux intensities. Owing to the flow restriction, the sonic approximation yields rather high blanket densities at high flux values. Removal of the sonic constraint yields Mach numbers of the order of unity at low flux values, but rather high Mach numbers at reactor conditions. The corresponding ablation rates vary acocordingly: at low flux values the two approximations yield results of the same order of magntidue, which are also in agreement with experimental observations[1,2]; at high flux values, owing to the rather high inherent blanket densities, the sonic approximation yields ablation rates that are of 2 orders of magnitude higher than those obtained with the momentum balance. Considering experimental installations of the type of ASDEX in Garching ($\phi_o \gtrsim 10^{11}$) or larger, the ablation times corresponding to the momentum blanace approximation would require pellet injection speeds of the order of 10^3 to 10^4 m/s.

It should be noted that the assumptions leading to the ablation rates desplayed in Tables 2 and 3 are rather optimistic: computations performed with vapor velocities v_{vap} greater than the sonic velocity at the pellet temperature yield higher ablation rates. Diamagnetic effects may cause an additional increase of the estimated rates. For example, if in the momentum balance approximation equ. (2.33) is replaced by equs. (2.32) and (2.34), for the case with $\phi = 10^{11}$ w/m^2, $B_{vac} = 3$ T, and $r_p = 0.52$ mm (ASDEX-conditions)

the following set of ablation parameters is obtained: $r_1 = 5.6$ mm, $n_1 = 3.2 \times 10^{17}$ (cm^{-3}), $T_1 = 1.1$ eV, $\Delta\ell = 4.4$ mm, $M_1 = 4.7$, $G = 5.4 \times 10^{24}$ s^{-1}, and $\tau = 5.3$ μs. The functional relation among ϕ_o, n_1, T_1, and r_1 is qualitatively the same in all these approximations.

3. CONCLUSIONS

a) An alaysis of the kinetics of ablation waves requires a two-wave approximation: the effect of the shock wave preceeding the ablation wave cannot be generally neglected. The two-wave model has one free (unknown) flow parameter, which should be chosen in accordance with experimental observations.

b) The magnetic Reynolds number based on the parameters of the blanket surrounding the pellet plays an important role in the ablation process: it determines whether the blanket remains diamagnetic or becomes magnetized and thus affects the magnitude of the energy influx.

c) The field diffusion model presented here indicates that the ablation process may be self-regulating: higher energy influx is compensated by smaller blanket radius and higher blanket density, the blanket temperature of the order of 1 eV being practically independent of the energy flux value.

d) A self-consistent analysis of the ablation process should include the consideration of such phenomena as the interaction of the incident plasma particles with the blanket (penetration depths, energy deposition rates, etc.); the ionization, recombination and charge exchange processes in the blanket, the blanket-magnetic field interaction, and the ablation wave kinetics in the pellet. A simultaneous account for all these effects is likely to require properly posed numerical models.

REFERENCES

1 C.A. Foster, R.J. Colchin, and C.D. Hendricks, Bull. Am. Phys. Soc. Ser II, 2o, 1300 (Oct. 1975).

2 K. Büchl and R. Lang, Verhandlungen der Deutschen Phys. Gesellschaft, Spring Conference 1977, Essen, 3, 663 (1977).

3 L. Spitzer, Jr., D.J. Grove, W.E. Johnson, L. Tonks, and W.R. Westendrop, USAEC, Rept. N.Y.O.-6047 (1954).

4 R.Carruthers, Proc. Nucl. Fus. React. Conf. Culham, p. 337 (1969).

5 D.J. Rose, Culham Lab. Techn. Div. Memo. No. 82 (1968).

6 A. Dalgarno in Atomic and Molecular Processes (ed. D.R. Bates), Academic Press, N.Y. 1962.

7 C.T. Chang, Nucl. Fusion 15, 595 (1975).

8 S.L. Gralnick, (a) Nucl. Fusion 13, 703 (1973); (b) Ph.D. Thesis, Columbia University, N.Y.,1972, p. 35.

9 D. Düchs, IPP Garching Rep. 1/14 (1963).

10 D.R. Bates, A.E. Kingston, and. R.W. McWhirter, Proc. Roy. Soc., Ser. A, 267, 297 (1962).

11 L.L. Lengyel, Pl. Phys. 18, 929 (1976).

12 S.J. Gitomer, R.L. Morse, and B.S. Newberger, Phys. Fluids 20, 234 (1977).

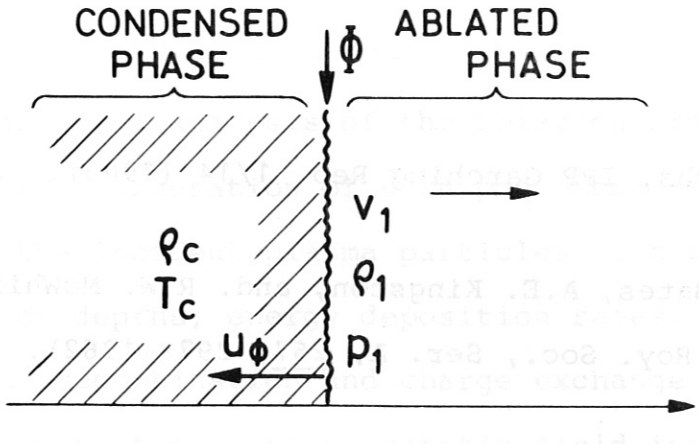

Fig.1 TWO-PHASE ABLATION MODEL

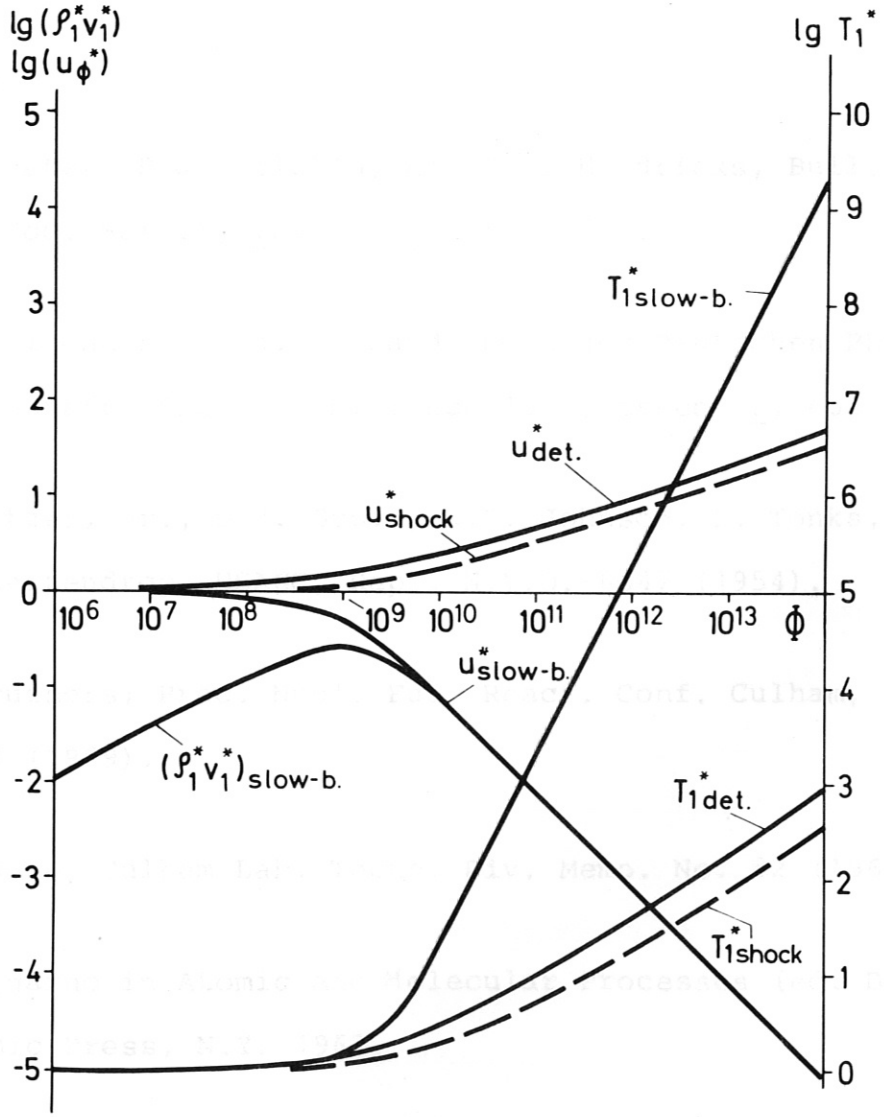

Fig. 2 TWO-PHASE ABLATION MODEL: PARAMETER VARIATIONS VS INCIDENT ENERGY FLUX Φ (w/m^2). $T_{ref} = 10°K$, $u_{ref} \approx 262$m/s

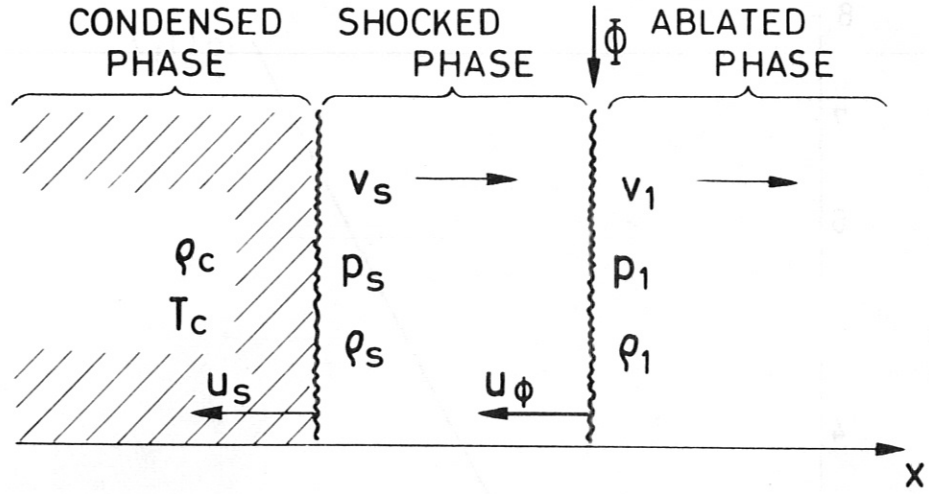

Fig.3 THREE-PHASE ABLATION MODEL

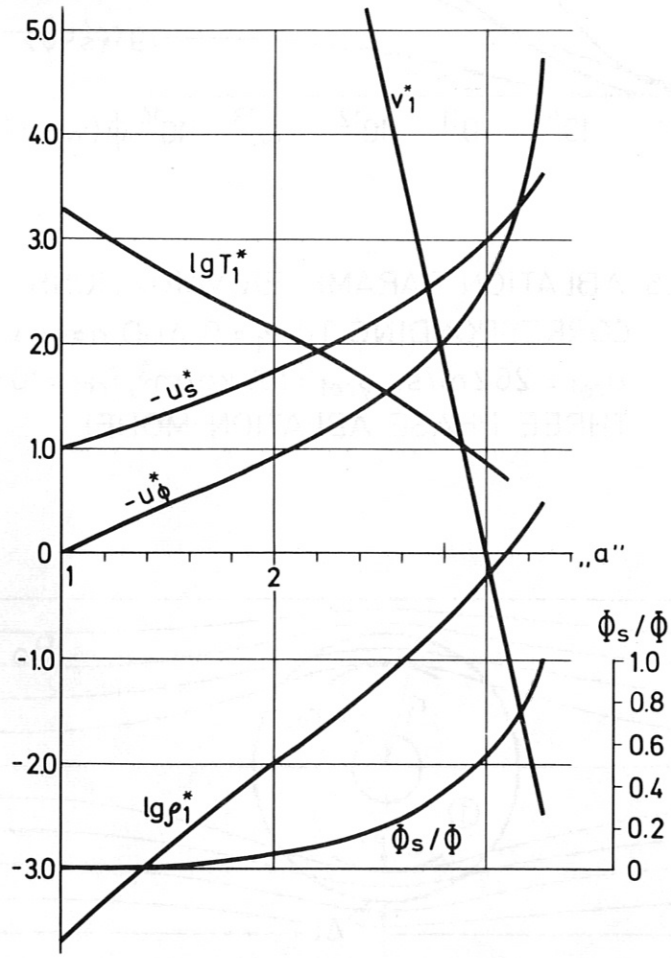

Fig.4 ABLATION PARAMETER VARIATIONS AS FUNCTIONS OF THE COMPRESSION RATIO „a" FOR $\Phi = 10^{11}\,w/m^2$, $T_{ref} = 10^0 K$, $u_{ref} \approx 262\,m/s$, $\rho_{ref} \approx 167\,kg/m^3$

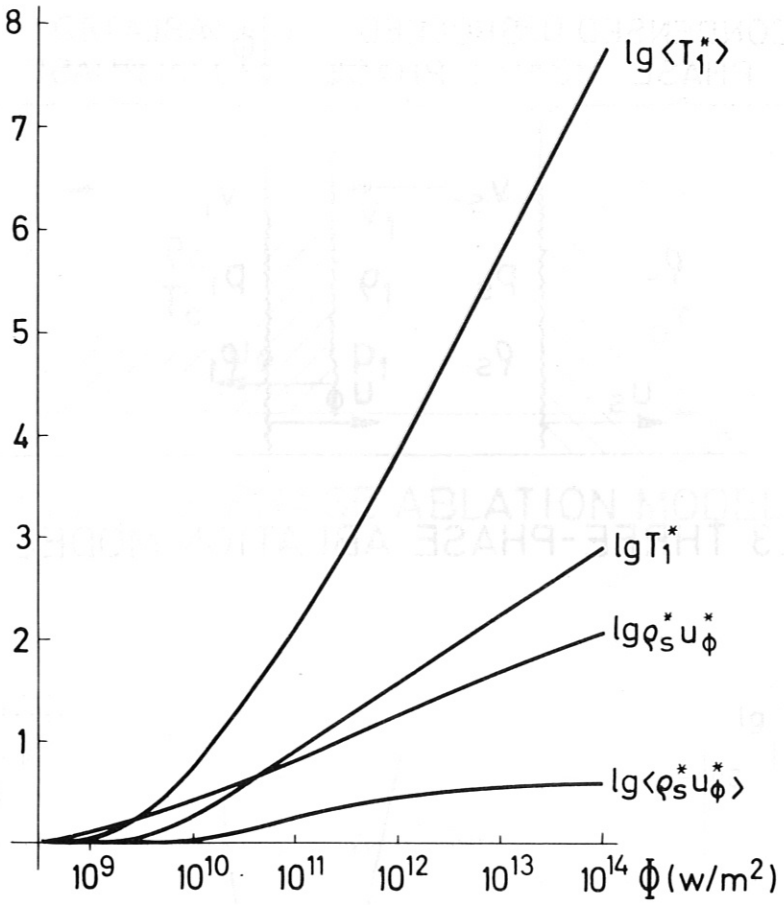

Fig.5 ABLATION PARAMETER VARIATIONS CORRESPONDING TO $v_1 = 0$ AND $a = \langle a \rangle$.
$u_{ref} = 262\,m/s$, $\rho_{ref} = 167\,kg/m^3$, $T_{ref} = 10°K$.
THREE PHASE ABLATION MODEL.

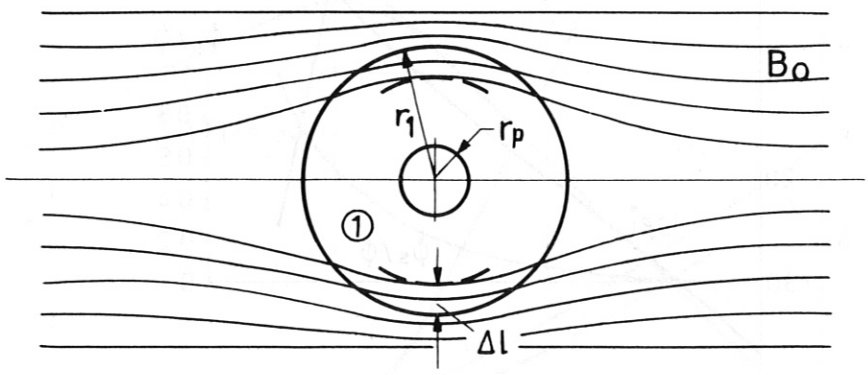

Fig.6 PELLET ABLATION IN MAGNETIC FIELD